Synthesis and Characterization of Barium Ferrite Containing Magnetic Affinity Microbeads and Isotherm Analysis of Cr(VI) Ions Adsorption from Aqueous Solutions

Baryum Ferit İçeren Manyetik Afinite Mikroküreleri Sentezi, Karakterizasyonu ve Sulu Çözeltilerden Cr(VI) İyonlarının Adsorpsiyon İzotermlerinin Analizi

Research Article

Ali Kara[1*], Emel Demirbel[1], Hüseyin Sözeri[2], İlker Küçük[3], Hüseyin Ovalıoğlu[3]

[1]Department of Chemistry, Uludağ University, Bursa, Turkey.

[2]TUBITAK-UME, National Metrology Institute, Gebze, Kocaeli, Turkey

[3]Department of Physics, Uludağ University, Bursa, Turkey

ABSTRACT

In this study, barium ferrite ($BaFe_{12}O_{19}$) containing metal-chelate microbeads, hard-mag-poly(ethylene glycol dimethacrylate-n-vinyl imidazole) [h-mag-poly(EGDMA–VIM)] (average diameter 53–212 μm), were synthesized and characterized. Their usage as an adsorobent in removal of Cr(VI) ions from aqueous solutions was investigated. The h-mag-poly(EGDMA–VIM) microbeads were prepared by copolymerizing of ethylene glycol dimethacrylate (EGDMA) with n-vinyl imidazole (VIM) and were characterized by elemental analysis, scanning electron microscopy, X-ray powder diffractometry vibrating magnetization measurements and swelling studies. The adsorption potential of microbeads for Cr(VI) ions from aqueous solutions was investigated. They exhibited the highest Cr(VI) ions adsorption capacity at pH 2.0 and adsorbent dosage of 50 mg. To predict the adsorption isotherms and to determine the characteristic parameters for process design, seven single and two parameter isotherm models were applied to experimental data. Three error analysis methods were used to evaluate the experimental data. Correlation coefficient, standard error, and sum of squares error of the estimate were to find the best fitting isotherm.

Key Words

Magnetic polymers; adsorption isotherms; Cr(VI) ions.

ÖZET

Sunulan bu çalışmada, barium ferrit içeren sert-manyetik-poli(etilen glikol dimetakrilat-n-vinil imidazol) [h-mag-poly(EGDMA–VIM)] metal-şelat mikroküreleri (ortalama çap 53-212 μm) sentezlendi ve karakterize edildi. h-mag-poly(EGDMA–VIM) mikroküreleri etilen glikol dimetakrilat ile n-vinil imidazolün kopolimerizasyonu ile hazırlandı ve elementel analiz, taramalı elektron mikroskobu, titreşimli mıknatıslanma ölçümleri ve şişme çalışmalarıyla karakterize edildi. Sulu çözeltilerden Cr(VI) iyonları için mikroküreleri adsorpsiyon potansiyelleri araştırıldı. pH=2 ve adsorbent miktarı=50 mg'da en yüksek Cr(VI) adsorpsiyon kapasitesi elde edildi. Adsorpsiyon izotermlerini tahmin etmek ve karakteristik parametrelere karar vermek için yedi tek ve ikili parametre izoterm modelleri uygulandı. Üç hata analiz yöntemi, korelasyon katsayısı, standart hata ve hata kareleri toplamı, en uygun izotermi bulmada deneysel verileri değerlendirmek için kullanıldı.

Anahtar Kelimeler

Manyetik polimerler, adsorpsiyon izotermleri, Cr(VI) iyonları

Article History: Received: Jan 1, 2014; Revised: Jun 19, 2014; Accepted: Aug 29, 2014; Available Online: Sep 15, 2014.

Correspondence to: Department of Chemistry, Uludağ University, Bursa, Turkey.

Tel: +90 224 2941733 Fax: +90 224 2941899 E-Mail: akara@uludag.edu.tr

INTRODUCTION

Chromium has applications in a variety of industries such as leather tanning, pigment manufacture, textile and dyeing [1]. The most common oxidation states of chromium are from +2 to +6, but only two states, +3 and +6, are of environmental significance. However, Cr(VI) ions are 500 times more toxic than the trivalent ones and human toxicity of chromium includes skin irritation to lung cancer, as well as kidney, liver, and gastric damage [2]. Several treatment processes have been in practice for removal of Cr(VI) ions from water and wastewater. Reduction of Cr(VI) ions to Cr(III) by a reducing agent and precipitation of chromium by pH adjustment has been quite popular [3]. Removal of Cr(VI) by adsorption onto polymer has been a popular choice nowadays [4]. Polymeric adsorbents have some significant advantages in the preparation of carrier matrix. For instance, polymeric adsorbents can be readily produced in a wide range of physicochemical properties (size, size distribution, porosity, hydrophobicity, etc.) and they are modifiable by inserting various ligands into the structure to make them sensitive to specific elements [5]. Polymeric adsorbents are generally preferred for the removal of Cr(VI) due to their high efficiency, easy handling, availability of different adsorbents, reusability, and cost effectiveness.

Polymeric microbeads with different properties can be easily be produced and converted into specific adsorbents by introducing different metal-complexing ligands. Thus, metal-complexing ligands in polymeric microbeads such as dithiocarbamate [6,7], dithizone [8], vinyl pyridine [9], phenylenediamine [10,11], chitosan [12]), vinyl imidazole [13,14], diethylenetriamine [15], N-methacryloylhistidine [16], poly(ethyleneimine) [17,18], salicylaldoxime [19], tannic acid [20] and vinyl triazole [21] have been used for the removal of heavy metal ions.

Magnetic polymeric beads are currently enjoying a fairly ample range of applications in many fields including biotechnology, nanotechnology and biochemistry [22-27]. Their magnetic feature makes sampling and collection of waste water (or pollutants) easier and faster. Magnetic microbeads are commonly manufactured from polymers since they have a variety of surface functional groups which can be tailored to use in specific applications. Different polymeric magnetic beads are used in the removal of Cr(VI) ions applications [28-30].

Adsorption isotherm equations, which explain the process at equilibrium conditions, provide an easier solution to complicated problems such as external mass transfer of solute, intraparticle diffusion, and adsorption at sites. Unless extensive data are available, it is impossible to predict the rate-determining step involved in the process. Therefore, the most appropriate method in designing the adsorption systems and in assessing the performance of the adsorption systems is to have an idea on adsorption isotherms. Langmuir and Freundlich models (two-parameter models) are the most commonly used isotherms. Simplicity and easy interpretability are some of the important reasons for extensive use of these models [31]. Moreover, linear regression has been frequently used to evaluate the model parameters. However, transformations of nonlinear isotherm equations to linear forms usually result in parameter estimation error and distort the fit [32,33]. Thus, a nonlinear method is a better way to obtain the equilibrium isotherm parameters. Most of the published literature had used two or three isotherm models, mainly Freundlich, Langmuir, and Dubinin-Radushkevich. In the present work, an attempt has been made to test most of the available isotherm models with the sorption data obtained. Considering these, the efficacy of h-mag-poly(EGDMA–VIM) for the removal of Cr(VI) was assessed using the best fit of single parameter model developed by Henry [34], two parameter models by Freundlich [35], Langmuir [36], Dubinin-Radushkevich (DR) [37], Temkin [38] and Halsey [39], three-parameter models by Redlich-Peterson [40], Sips [41], Khan [42], Radke-Prausnitzr [43], Toth [44] and Koble-Carrigan [45], four- and five-parameter models by Fritz and Schlunder [46] isotherms in their nonlinear form.

In this study, we synthesized and characterized the h-mag-poly(EGDMA–VIM) microbeads. We show that the h-mag-poly(EGDMA–VIM) microbeads can be used directly for adsorption of Cr(VI) ions from aqueous solutions. In order to clarify the adsoption process, we have conducted different isothermal analysis.

MATERIALS AND METHODS

Materials

Ethylene glycol dimethacrylate (EGDMA) was obtained from Merck (Darmstadt, Germany), purified by passing through active alumina and stored at 4°C until use. N-Vinyl imidazole (VIM, Aldrich, Steinheim, Germany) was distilled under vacuum (74–76°C, 10 mmHg). 2,2′-Azobisisobutyronitrile (AIBN) was obtained from Fluka A.G. (Buchs, Switzerland). Poly(vinyl alcohol) (PVAL; Mw: 100.000, 98% hydrolyzed) was supplied from Aldrich Chem. Co. (USA). All other chemicals were of reagent grade and were purchased from Merck AG (Darmstadt, Germany). All water used in the binding experiments was purified using a Barnstead (Dubuque, IA) ROpure LPw reverse osmosis unit with a high flow cellulose acetate membrane (Barnstead D2731) followed by a Barnstead D3804 NANOpurew organic/colloid removal and ion exchange packed-bed system. Buffer and sample solutions were prefiltered through a 0.2 mm membrane (Sartorius, Göttingen, Germany). All glassware was extensively washed with dilute nitric acid before usage.

Synthesis of Barium Hexaferrite ($BaFe_{12}O_{19}$) nanoparticles

Appropriate amounts of $BaCO_3$ and Fe_2O_3 powders were weighted to prepare barium hexaferrite in a nominal composition (i.e., Fe:Ba ratio is 12:1). Starting materials were mixed, while heating at 100°C, in 1 M nitric acid solution (pH 0.5) by using magnetic stirrer. For 5 g of initial powders, 100 ml acid was used. Mixing was continued until dry precursor was obtained. Before grinding in an agata mortar for 15 min, small amount of ethyl alcohol was added to make wet grinding. Then, the precursor was calcinated at 450°C for 4h to remove possible organic compounds. Finally, the precursor was pelletized under the pressure of 200 MPa before annealing at 1000°C for 2h.

Preparation of the h-mag-poly(EGDMA-VIM) microbeads

In order to prepare h-mag-poly(EGDMA–VIM) microbeads for Cr(VI) adsorption, suspension polymerization technique was used. EGDMA and VIM were polymerized in suspension by using AIBN and poly(vinyl alcohol) as the initiator and the stabilizer, respectively. Toluene was included in the polymerization recipe as a diluent (as a pore former). A typical preparation procedure was examplified below. Continuous medium was prepared by dissolving poly(vinyl alcohol) (200 mg) in the purified water (50 ml). For the preparation of dispersion phase, EGDMA (6 ml; 30 mmol), magnetic barium ferrite nanopowder (0.5 g) and toluene (10 ml) were stirred for 15 min at room temperature. Then, VIM (3 ml; 30 mmol) and AIBN (100 mg) were dissolved in the homogeneous organic phase, which was dispersed in the aqueous medium by stirring the mixture at 400 rpm in a sealed cylindrical pyrex polymerization reactor. The reactor content was heated to polymerization temperature (i.e., 70°C) within 4 h and the polymerization was conducted for 2 h with a 600 rpm stirring rate at 90°C. Finally, beads were washed with ethanol and water several times to remove any unreacted monomer or diluent. Then, they were dried at 50°C in vacuum oven. The magnetic beads were sieved to different sizes and microscopic inspection shows that almost all the beads are perfectly spherical.

Characterization of the h-mag-poly(EGDMA-VIM) microbeads

To evaluate the degree of VIM incorporation, the h-mag-poly(EGDMA–VIM) microbeads were subjected to elemental analysis with a Leco elemental analyzer (model CHNS-932, St. Joseph, MI). The specific surface area of the polymeric microbeads was determined in a Brunauer Emmet Teller (BET) isotherm of nitrogen with an ASAP2000 instrument (Micromeritics). The average size and size distribution of the beads were determined by screen analysis performed with Tyler standard sieves (Retsch Gmbh; Haan, Germany). The water uptake ratio of the h-mag-poly(EGDMA–VIM) microbeads was determined in distilled water. The experiment was performed as follows. Initially, dry beads were carefully weighed before they were placed in a 50-mL vial containing distilled water. The vial was put into an isothermal water bath with a fixed temperature (25 ± 0.5°C) for 2 h. The bead sample was taken from the water, wiped with filter paper, and weighed. The mass ratios of dry and wet samples was recorded. The surface morphology and

internal structure of the h-mag-poly(EGDMA–VIM) microbeads were observed via a scanning electron microscope (Jeol, JEM 1200EX, Tokyo). The h-mag-poly(EGDMA–VIM) microbeads were dried at room temperature and coated with a thin layer of gold (ca. 100 Å) ***in vacuo*** and photographed in the electron microscope with 1000X magnification. The magnetic characterization of the samples, all in powder form, was performed at room temperature using a vibrating sample magnetometer (VSM) (LDJ Electronics Inc., Model 9600) in an applied field of 15 kOe. X-ray powder diffraction (XRD) analysis was conducted on a Rigaku-Minflex diffractometer with Cu-K_α radiation.

Batch adsorption experiments

Batch adsorption experiments were performed by using 50 mg of the h-mag-poly(EGDMA–VIM) microbeads with 50 ml of aqueous metal ion solutions in 100 cm^3-erlenmeyer flasks, of which concentrations, pH and temperature have already been known. The sample was shaken at 300 rpm in a shaking water bath (Clifton, England). After desired contact time, suspension was filtered. The filtrate was analyzed for metal ions by using an UV-vis spectrophotometer (Shimadzu-2100 UV-vis, Japan).

Nonlinear Regression Analysis

All the model parameters were evaluated by nonlinear regression using SPSS (Ver.17).

The optimization procedure requires an error function to be defined in order to be able to evaluate the fit of the equation to the experimental data [47]. Apart from the correlation coefficient (R^2), the sum of squares error (SSE) and the standard error (SE) of the estimate were also used to measure the goodness-of-fit can be defined as:

$$SE = \sqrt{\frac{1}{m-p}\sum_{i=1}^{m}(Q_i - q_i)^2}$$

SSE can be defined as:

$$SSE = \sum_{i=1}^{m}(Q_i - q_i)^2$$

where, q_i is the observation from the batch experiment, Q_i is the estimate from the isotherm for corresponding q_i, m is the number of observations in the experimental isotherm, and p is the number of parameters in the regression model. Small values indicate that fitting is well.

Desorption and repeated use

Cr(VI) ions bound to the microbeads in 1.0 M HNO_3 and 1.0 M NaOH solutions was desorbed in a shaking water bath at 300 rpm for 24 h at room temperature. The final Cr(VI) ions concentration in the desorption medium was determined by UV-vis spectrophotometer. The desorption ratio was calculated from the amount of Cr(VI) adsorbed on the microbeads and the final Cr(VI) concentration in desorption medium, by using the following expression.

$$\text{Desorption ratio} = \frac{\text{Amount of Cr(VI)ions desorbed to the desorption medium}}{\text{Amount of Cr(VI)ions adsorbed on the microbeads}} x10 \quad (1)$$

In order to determine the re-usability of the hard magnetic microbeads, consecutive adsorption-desorption cycles were repeated ten times by using the same magnetic microbeads.

RESULTS AND DISCUSSION

Properties of porous polymer microbeads

The suspension polymerization procedure provided crosslinked h-mag-poly(EGDMA–VIM) microbeads in a spherical form within a size range of 53–212 μm. To investigate the surface morphology and bulk structure of the beads, SEM micrographs were analyzed (Figure 1). The polymeric beads had a rough surface. The roughness of the surface probably caused an increase in the surface area. The morphology changed because of the barrium ferrite existance in the h-mag-poly(EGDMA–VIM) microbeads which was clearly seen from the SEM image. Specific surface area of h-mag-poly(EGDMA–VIM) microbeads were found to be 81.4 m^2/g. The microbeads are crosslinked gels and can not be dissolved in an aqueous medium, but do swell, depending on the degree of cross-linking. The equilibrium swelling ratio for the microbeads are 83%. In addition, they have highly cross-linked and strong structure which makes these beads useable for column applications.

To evaluate the degree of VIM incorporation into the polymeric structure, elemental analysis

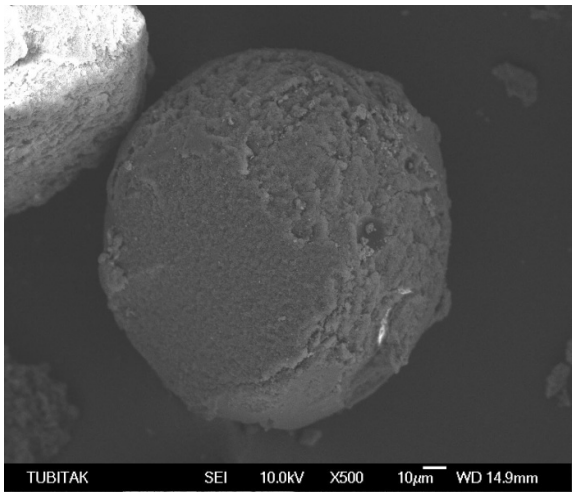

Figure 1. Scanning electron micrograph of the h-mag-poly(EGDMA-VIM) microbeads.

Table 1. VIM and $BaFe_{12}O_{19}$ determination in h-mag-poly(EGDMA-VIM) with elemental analysis.

C%	54.25
N%	8.73
H%	7.65
µmol VIM/g polymer	675.7
$BaFe_{12}O_{19}$%	16.7

of the synthesized microbeads was performed (Table 1). The resulting nitrogen stoichiometry indicated that 675.7 µmol VIM/g polymer had been incorporation in the microbeads. This indicates that most of the VIM charged into reactor has been successfully incorporated into the microbeads by the polymerization procedure applied.

The average $BaFe_{12}O_{19}$ content of the h-mag-poly(EGDMA-VIM) microbeads was determined by density analysis [27]. The hydrated density of the h-mag-poly(EGDMA-VIM) microbeads measured at 25°C was 1.83 g/mL. By the same procedure, the density of $BaFe_{12}O_{19}$ particles was found to be 5.26 g/ml at 25°C and that of non-magnetic microbeads was found to be 1.14 g/mL. The magnetic particles volume fraction in the h-mag-poly(EGDMA-VIM) microbeads can be calculated from the following equation derived from the mass balance:

$$\emptyset = (\rho_C - \rho_M)/(\rho_C - \rho_A) \quad (2)$$

where, ρ_A, ρ_C and ρ_M are the densities of non-magnetic microbeads, $BaFe_{12}O_{19}$ nanopowder, and

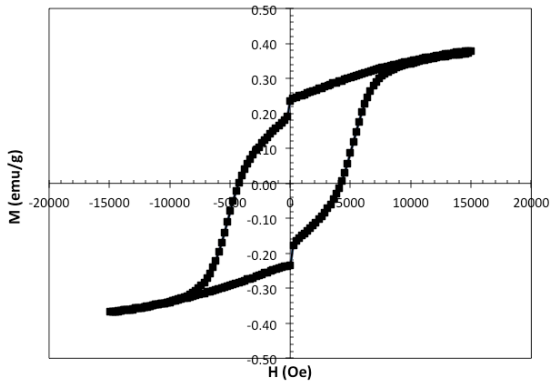

Figure 2. M-H curve of magnetic evaluation of h-mag-poly(EGDMA-VIM) microbeads.

magnetic microbeads, respectively. Thus, with the density data mentioned above, the h-mag-poly(EGDMA-VIM) microbeads gel volume fraction in the magnetic beads was estimated to be 83.3%. Therefore, the average $BaFe_{12}O_{19}$ content of the resulting magnetic microbeads is 16.7%.

The characterization of the microbeads was performed with magnetization measurements. Figure 2 shows the M-H curve at room temperature which exhibites a hysteretic behaviour with quite high coercivity of nearly 4 kOe. In addition, the intensities of broad diffraction peaks corresponding to $BaFe_{12}O_{19}$ in the poly(EGDMA-VIM) microbeads become weakened with increasing the amount of poly(EGDMA-VIM). These results show that mag-poly(EGDMA-VIM) has a hard magnetic behavior and the magnetic performance of the material is important for their promising uses.

Adsorption of Cr(VI) ions

Effect of pH on the adsorption of Cr(VI) ions

The adsorption of the metal ions onto an adsorbent varies generally with pH, since it changes the radius of hydrolyzed cation and charge of the adsorbent surface. Therefore, in this study, the adsorption of Cr(VI) ions onto the microbeads studied as a function of pH. The initial pH values of Cr(VI) solutions were kept between 2.0 and 6.0. The relationship between initial pH and the amount of Cr(VI) adsorbed on the h-mag-poly(EGDMA-VIM) microbeads for initial solution concentrations of 50 mg.dm^{-3} for at 25°C and a contact time of 250 min is illustrated in Figure 3. When initial pH values of Cr(VI) solutions

are increased from 2.0 to 6.0, the amounts of Cr(VI) adsorbed per unit mass of adsorbent are decreased. For example, amount of Cr(VI) ions adsorbed per unit adsorbent decrease from 16.20 to 0.00 mg.g^{-1} for Cr(VI) ions when the pH value increase from 2.0 to 6.0. As seen in the Figure 3, pH 2 is a value for the maximum adsorption of Cr(VI) ions. The adsorption of Cr(VI) ions depends on the protonation or unprotonation of functional groups on surface of the microbeads. Cr(VI) ions exists in anionic forms (i.e. $Cr_2O_7^{2-}$, $HCrO_4^-$, CrO_4^{2-} and $HCr_2O_7^-$) in aqueous medium, and fraction of any particular species is depend on chromium concentration and pH [12]. At acidic pH, the imidazole groups of the microbeads are positively charged, which leads to an electrostatic attraction for the negatively charged chromium species. The fact that a rise in the pH cause to the decrease of the adsorption of metal ions is attributed that protonation of imidazole groups on the h-mag-poly(EGDMA-VIM) microbeads has become more positive.

Effect of adsorbent dosage on adsorption of Cr(VI) ions

The effect of adsorbent dosage on the adsorption of Cr(VI) ions is shown in Figure 4. The percentage removal increases from 32.0 to 96.8% by increasing the adsorbent dosage from 50 to 800 mg. It is apparent from Figure 6 that by increasing the resin amount, adsorption efficiency increases but adsorption density, amount adsorbed per unit mass, decreases. It is readily understood that the number of available adsorption sites increases by increasing the adsorbent amount. However, the decrease in adsorption capacity is basically due to the sites remaining unsaturated during the adsorption process [49-53].

Isothermal analysis on adsorption of Cr(VI) ions

The relationship between the amount of Cr(VI) ions adsorbed onto the adsorbent surface and the remaining Cr(VI) ions concentration in the aqueous phase at equilibrium can be observed by the adsorption equilibrium isotherm analysis

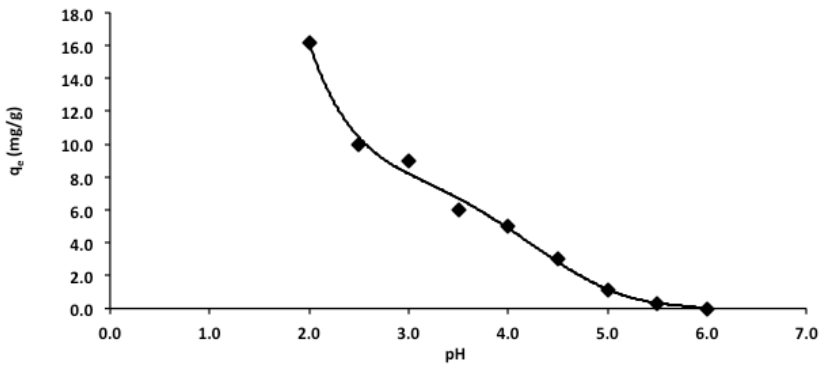

Figure 3. Effect of pH on adsorption of Cr(VI) ions of the h-mag-poly(EGDMA-VIM) microbeads.

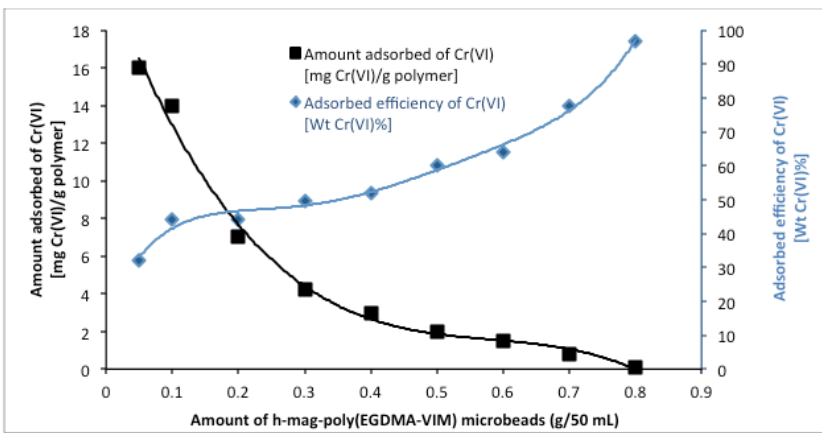

Figure 4. Effect of adsorbent dosage on adsorption of Cr(VI) ions in 50 mL of solution containing 50 mg/L Cr(VI) ions at pH: 2.0; T: 298 K.

as shown in investigate the effect of initial concentration of Cr(VI) ions. This relationship showed that the adsorption capacity increased with the equilibrium concentration of the Cr(VI) ions in solution, progressively reaching saturation of the adsorbent. Adsorption isotherm curves indicates that adsorption phenomenon may be represented by isotherms of type I which represent a monolayer adsorption until the saturation of active sites. To predict the adsorption isotherms and to determine the characteristic parameters for process design, seven single and two parameter isotherm models-Henry's law, Freundlich, Langmuir, Dubinin-Radushkevich, Temkin and Halsey-six three-parameter equations-the Redlich-Peterson, Sips, Khan, Radke-Prausnitz, Toth, and Koble-Corrigan-and four- and five-parameter isotherm equations of Fritz and Schluender isotherm models were applied to experimental data. (Table 1 and 2). Three error analysis methods were used to evaluate the experimental data, viz. correlation coefficient, standard error (SE), and sum of squares error (SSE) of the estimate, to find the best fitting isotherm.

Among the isotherm models considered in the present study, Henry's law is the simplest

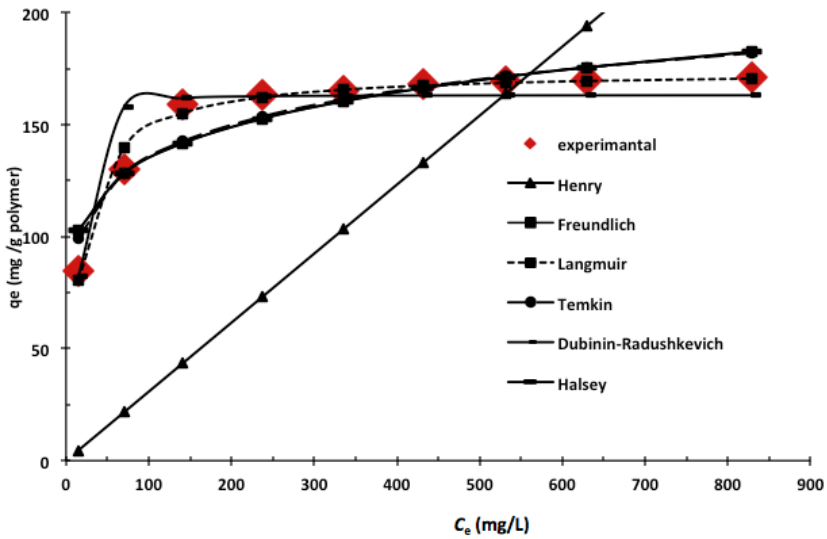

Figure 5. Application of one- and two-parameter models to experimental isotherm data obtained for Cr(VI) adsorption onto h-mag-poly(EGDMA-VIM) microbeads.

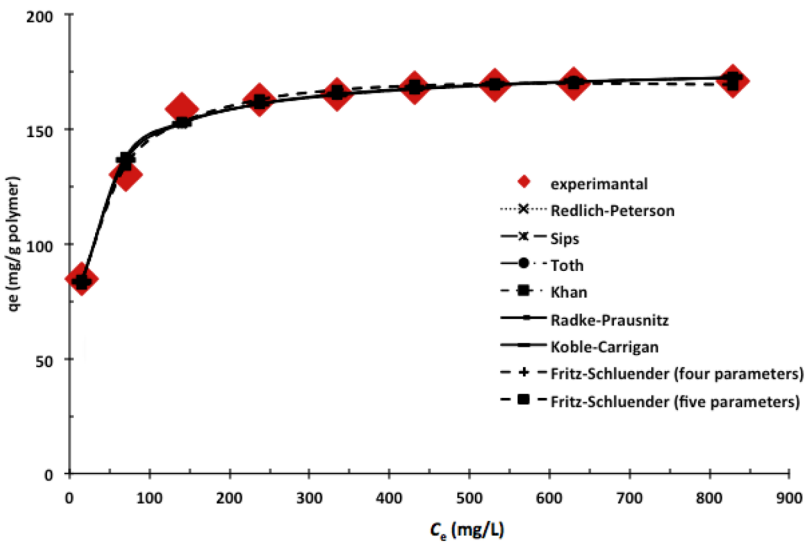

Figure 6. Application of three-, four-, and five-parameter models to experimental isotherm data obtained for Cr(VI) adsorption onto h-mag-poly(EGDMA-VIM) microbeads.

one having a single parameter, and it has been successfully applied in many cases [54]. The Henry's law model is applied to describe the experimental data obtained for the adsorption of Cr(VI) onto our microbeads. Figure 3, as well as , and values (see Table 2) indicate that this model completely fails to predict the equilibrium isotherm in the present case. This may be due to the unavailability of adsorption data in the lower range of Cr(VI) concentration. The Freundlich isotherm is originally empirical in nature [9] but was later interpreted for adsorption to heterogeneous surfaces or surfaces supporting sites of varied affinities and has been used widely to fit experimental data [55]. The value of ***n***, of this model, falling in the range of 1–10 indicates favorable sorption [56]. The present study results (Table 2) indicate that the Freundlich model (Freundlich 1906) also is unable to give a good fit to the equilibrium data as evidenced by the low correlation coefficient, though the values of and are low and the adsorption is also favorable as the ***n*** value is in the range of 1–10. The Langmuir model (Langmuir 1916) served to estimate the maximum metal uptake values where they could not be

Table 2. Single and three-parameter adsorption isotherm models.

Isotherm models	equation	parameters	remarks	confirmations
Henry	$q_e=K_{HE}\,C_e$	K_{HE} (L/g)=0.308 R^2=0.891 SE=0.0809 SSE=52.44	very simple expression applicable at low effluent concentration	R^2, SE and SSE values indicate that the Henry model completely fails to predict the equilibrium isotherm in the present case.
Freundlich	$q_e=K_F\,Ce^{(1/n)}$	K_F (L/g)=69.74 n_F=6.983 R^2=0.963 SE=0.011 SSE=0.922	simple expression not structured, no leveling off	The Freundlich model also was unable to give a good fit to the equilibrium data as evidenced by the low correlation coefficient, though the values of SE and SSE were low.
Langmuir	$q_e=(q_m\,K_L\,C_e)/(1+K_L\,C_e)$ $R_L=1/(1+K_L\,C_i)$	K_L (L/mg)=0.058 q_m (mg/g)=174.3 R_L=0.017-0.257 R^2=0.995 SE=0.004 SSE=0.126	simple expression and interpretable parameters not structured; monolayer sorption	The experimental data fit the Langmuir isotherm very well with a high value of R^2 and low SE and SSE values.
Dubinin-Radushkevich	$q_e=q_m\,\exp\alpha(-\beta e^2)$ $e=RT\,\ln(1+1/C_e)$	β (mol^2/kJ^2)=42.28 q_m (mg/g)=163.1 R^2=0.961 SE=0.012 SSE=0.965	temperature-independent and suitable for porous adsorbent	The Dubinin-Radushkevich model also was unable to give a good fit to the equilibrium data as evidenced by the low correlation coefficient, though the values of SE and SSE were low.
Temkin	$q_e=\ln(K_{Te}\,C_e)^{B_{Te}}$	K_{Te} (L/g)=3.530 b_{Te} (J/mol)=111.8 R^2=0.970 SE=0.010 SSE=0.741	simple expression no special advantage	The Temkin model also was unable to give a good fit to the equilibrium data as evidenced by the low correlation coefficient, though the values of SE and SSE were low.
Halsey	$q_e=\alpha(K_H/C_e)^{1/n_H}$	n_H=6.985 R^2=0.963 SE=0.012 SSE=0.922	calculates adsorption energy multilayer adsorption	The Halsey model also was unable to give a good fit to the equilibrium data as evidenced by the low correlation coefficient, though the values of SE and SSE were low.

reached in the experiments, and it contains the two important parameters of the adsorption system and is attributable to the maximum metal uptake upon complete saturation of the adsorbent, and is a coefficient attributed to the affinity between the adsorbent and adsorbate. The experimental data fit the Langmuir isotherm very well (Table 2) with a high value of and low and values. The separation factor values indicate (Table 1) that Cr(VI) onto the microbeads is favourable [57]. The Dubinin–Radushkevich, Temkin, and Halsey models were unable to describe the data well when compared with the other two-parameter models, as low correlation coefficients despite low and values, were observed. Figure 5 shows the application of all two-parameter models in the nonlinear form. It can be observed that the predicted Langmuir isotherm curve fits best. Upon comparing all the isotherm models, the isotherm curve predicted by the Langmuir model coincides with the experimental curve with a high correlation coefficient and low and values. Redlich and Peterson incorporated the features of the Langmuir isotherm into a single equation. There are two limiting behaviors: Langmuir form for and Henry's law form for. It is worth noting that the value is 0.979, i.e., the data can preferably be fitted with the Langmuir model. This is confirmed by the satisfactory fit of the data to the Langmuir model. At low adsorbate concentrations, Sips isotherm effectively reduces to the Freundlich isotherm and thus does not obey Henry's law. At high adsorbate concentrations, it predicts a monolayer adsorption capacity characteristic of the Langmuir isotherm. The exponent value was found to be 0.837; this means that the Cr(VI) adsorption data obtained in this study is more of the Langmuir form rather than that of Freundlich, which was also confirmed by the results shown in Table 2. The predicted values of by the Khan (Table 2) are comparable and lower as compared to Langmuir model for the present data, indicating the satisfactory fit of the Langmuir model. The Cr(VI) adsorption data correlates well with the Radke–Prausnitz isotherm model as well as the Toth and Koble–Carrigan isotherm model and this is confirmed by high correlation coefficients and low and values. The adsorption data were analyzed according to the nonlinear form of the Fritz–Schlunder (FS) four-parameter isotherm model and the Fritz–Schluender (FS) five-parameter model. An appropriate fitting of the experimental results of adsorption isotherms was obtained using the four-parameter model of Fritz–Schlunder and the five-parameter model of Fritz–Schlunder (Figure 6) as substantiated by a reasonably high coefficient of correlation (0.997) and low SE and SSE values (Table 2).

Desorption and repeated use

The use of an adsorbent in the adsorption process depends not only on the adsorptive capacity, but also on how well the adsorbent can be regenerated and used again. For repeated use of an adsorbent, adsorbed metal ions should be easily desorbed under suitable conditions. Desorption of the adsorbed Cr(VI) ions from the h-mag-poly(EGDMA-VIM) microbeads was also studied in a batch experimental system. Desorption experiments put into evidence that after 2 hours contact NaOH solutions (1.0 mol/L, desorption percentage 93%) were more efficient than HCl solutions (1.0 mol/L, desorption percentage 36%) to desorb Cr(VI) ions for the adsorbent. The repeated use for NaOH solutions of the h-mag-poly(EGDMA-VIM) microbeads shows that adsorption-desorption process is reversible process. Ten cycles of adsorption-desorption experiments were conducted to examine the capability of the h-mag-poly(EGDMA-VIM) microbeads to retain Cr(VI) ions removal capacity. The adsorption capacity of the h-mag-poly(EGDMA-VIM) microbeads was decreased only 6% during ten adsorption-desorption cycle.

ACKNOWLEDGEMENT

This work was partly supported by the Research Fund of The University of Uludag Project Number: KUOP(F)-2013/29 and Project Number: OUAP(F)-2012/28.

REFERENCES

1. S. Hena, Removal of chromium hexavalent ion from aqueous solutions using biopolymer chitosan coated with poly(3–methyl thiophene) polymer, J. Hazard. Mater. 181 (2010) 474.
2. A. Mansri, K.I. Benabadji, J. Desbrieres, J. Francois, Chromium removal using modified poly(4–vinyl pyridinium) bentonite salts, Desalination, 245 (2009) 95.

Table 3. Three-, four-, and five-parameter adsorption ısotherm models.

isotherm models	equation	parameters	remarks	confirmations
Redlich-Peterson	$qe=\{K_{RP}\ C_e\}/\{1 + a_{RP}\ C_e^{\beta_{RP}}\}$	K_{RP} (L/g)=11.34 a_{RP}=0.074 β_{RP}=0.979 R^2=0.995 SE=0.004 SSE=0.109	approaches Freundlich at high concentrations no special advantages Freundlich at high concentrations no special advantages	The experimental data fit the Redlich–Peterson isotherm very well with a high value of and low and values.
Sips	$q_e=\{q_m\ (K_s\ C_e\ )^{\gamma}\}/\{1+\ (K_s\ C_e\ )^{\gamma}\}$	K_S (L/g)=0.057 q_m (mg/g)=179.4 γ=0.837 R^2=0.996 SE=0.091 SSE=0.003	combination of Langmuir and Freundlich unnecessarily complicated	The experimental data fit the Sips isotherm very well with a high value of and low and values.
Khan	$q_e=\{q_m\ b_K\ C_e\}/\{(1+b_k\ C_e)^{a_K}\}$	a_K (L/g)=0.978 b_K (L/mg)=0.069 q_m (mg/g)=160.2 R^2=0.995 SE=0.004 SSE=0.111	another three parameter model	The experimental data fit the Khan isotherm very well with a high value of and low and values.
Radke-Prausnitz	$q_e=\{a_R\ r_R\ C_e^{\alpha}\}/\{a_R+r_R\ C_e^{\alpha-1}\}$	a_R (L/g)=11.33 r_R (L/mg)=0.153 α=20.11 R^2=0.995 SE=0.004 SSE=0.108	simple expression empirical, uses three parameters	The experimental data fit the Radke–Prausnitz isotherm very well with a high value of and low and values.

Table 3. Continued.

isotherm models	equation	parameters	remarks	confirmations
Toth	$q_e=\{q_m\ b_T\ C_e\}/\{[1+(b_T\ C_e)^{n}{}_T]^{1/n}{}_T\}$	b_T (L/g)=0.082 n_T=0.803 q_m (mg/g)=179.8 R^2=0.996 SE=0.003 SSE=0.093	improvement over Langmuir and Freundlich empirical, uses three parameters	The experimental data fit the Toth isotherm very well with a high value of and low and values.
Koble-Carrigan	$q_e=\{A_{KC}B_{KC}C_e{}^{n}{}_{KC}\}/\{1+B_{KC}C_e{}^{n}{}_{KC}\}$	A_{KC} (mg/g)=179.4 B_{KC} (L/g)=0.091 n_{KC}=0.836 R^2=0.996 SE=0.004 SSE=0.091	simple expression empirical, uses three parameters	The experimental data fit the Koble–Carrigan isotherm very well with a high value of and low and values.
Fritz-Schluender (four-parameter)	$q_e=\{AC_e{}^{\alpha}{}_{FS}\}/\{1+B_{FS}\ C_e{}^{\beta}{}_{FS}\}$	A=26.96 B_{FS}=0.042 α_{FS}=0.505 β_{FS}=0.668 R^2=0.997 SE=0.004 SSE=0.062	another Langmuir-Freundlich type uses four-parameters	The experimental data fit the Fritz–Schluender (four-parameter) isotherm very well with a high value of and low and values.
Fritz-Schluender (five-parameter)	$qe=\{a_1\ C_e{}^{\beta}{}_1\}/\{a_1{}'+a_2\ C_e{}^{\beta}{}_2\}$	a_1 (mg/g)=4.695 $a_1{}'$=0.174 a_2=0.007 β1=0.505 β_2=0.668 R^2=0.996 SE=0.004 SSE=0.002	improvement over Langmuir and Freundlich empirical, uses five parameters	The experimental data fit the Fritz–Schluender (five-parameter) isotherm very well with a high value of and low and values.

NOTATION

a_K	Khan model exponent
a_R	Radke-Prausnitz isotherm constant
a_{RP}	Redlich-Peterson model constant, L/mg
A	Fritz-Schluender four-parameter model constant
A_{KC}	Koble-Carrigan isotherm constant
b_K	Khan isotherm constant
b_T	Toth isotherm constant
b_{TE}	constant in Temkin adsorption isotherm, J/mol
B_{FS}	constant in Fritz-Schluender four-parameter model
B_{KS}	Koble-Carrigan isotherm constant
C_e	equilibrium concentration of adsorbate in solution, mg/L
e	Polanyi potential, kJ/mol
K_F	Freundlich isotherm constant,
K_{HE}	Henry's law constant,
K_H	Halsey isotherm constant
K_L	Langmuir isotherm equilibrium binding constant,
K_{RP}	RedlichPe-terson isotherm constant, L/g
K_S	Sips isotherm constant, L/g
K_{Te}	Temkin isotherm constant, L/mg
n_F	exponent in Freundlich isotherm
n_H	Halsey isotherm constant
n_{KC}	Koble+Carrigan model exponent
n_T	Toth isotherm constant
q_e	amount of adsorption at equilibrium, mg/g
q_i	observed adsorption capacity of batch experiment i
q_m	maximum adsorption capacity,
r_R	Radke-Prausnitz isotherm constant
R	universal gas constant, 8.314
R^2	correlation coefficient
R_L	Langmuir separation factor
SE	Standard error
SSE	Sum of squares error
α	Radke-Prausnitz isotherm constant
α_1	Fritz-Schluender 5-parameter model sorption capacity (mg/g)
α'_1	Fritz-Schluender five-parameter model constant
α_2	Fritz-Schluender five-parameter model constant
α_{FS}	Fritz-Schluender four-parameter model exponent
β	constant in Dubinin-Radushkevich sorption model,
β_1	Fritz-Schluender five-parameter model exponent
β_2	Fritz-Schluender five-parameter model exponent
β_{FS}	Fritz-Schluender four-parameter model exponent
β_{RP}	Redlich-Peterson isotherm constant
γ	Sips model exponent

3. N. Fiol, C. Escudero, I. Villaescusa, Chromium sorption and Cr(VI) reduction to Cr(III) by grape stalks and yohimbe bark, Bioresour. Technol., 99 (2008) 5030.
4. M. Owlad, M.K. Aroua, W. Ashri, W. Daud, S. Baroutian, Removal of Hexavalent Chromium– Contaminated Water and Wastewater: A Review Water Air Soil Pollut., 200 (2009) 59.
5. E. Uzdoğan, E.B. Denkbaş, O.S. Kabasakal, The use of polyethyleneglycol–methacrylate–co–vinylimidazole (PEGMA–co–VI) microspheres for the removal of nickel(II) and chromium(VI) ions J. Hazard. Mater., 177 (2010) 119.
6. R. Say, E. Birlik, A. Denizli, A. Ersöz, Heavy Metal Removal by Dithiocarbamate–Anchored Polymer/ Organosmectite Composites Appl. Clay Sci., 31 (2006) 298.
7. E. Pişkin, K. Kesenci, N. Şatıroğlu, Ö. Genç, Dithiocarbonate–incorporated monodisperse polystyrene microspheres as specific sorbents: adsorption of cadmium ions J. Appl. Polym. Sci., 59 (1996) 109.
8. B. Salih, A. Denizli, C. Kavaklı, R. Say, E. Pişkin, Adsorption of heavy metal ions onto dithizone–anchored poly(EGDMA–HEMA) microbeads, Talanta ,46 (1998) 1205.
9. A. Duran, M. Soylak, S.A. Tuncel, Poly(vinyl pyridine–poly ethylene glycol methacrylate–ethylene glycol dimethacrylate) beads for heavy metal removal,J. Hazard. Mater., 155 (2008) 114.
10. X.G. Li, X.L. Ma, J. Sun, M.R. Huang, Powerful reactive sorption of silver(I) and mercury(II) onto poly(o–phenylenediamine) microparticles, Langmuir, 25 (2009) 1675.
11. Q.F. Lu, M.R. Huang, X.G. Li, Synthesis and Heavy–Metal–Ion Sorption of Pure Sulfophenylenediamine Copolymer Nanoparticles with Intrinsic Conductivity and Stability, Chem. Eur. J., 13 (2007) 6009.
12. G.J. Copello, F. Varela, R.M. Vivot, L.E. Diaz, Immobilized chitosan as biosorbent for the removal of Cd(II), Cr(III) and Cr(VI) from aqueous solutions, Bioresour. Technol., 99 (2008) 6538.
13. A. Kara, L. Uzun, N. Beşirli¸ A. Denizli, Poly(ethylene glycol dimethacrylate–n–vinyl imidazole) beads for heavy metal removal, J. Hazard. Mater., 106B (2004) 93.
14. A. Kara, B. Erdem, Synthesis, characterization and catalytic properties of sulfonic acid functionalized magnetic–poly(divinylbenzene–4–vinylpyridine) for esterification of propionic acid with methanol, J. Mol. Catal. A: Chem., 349 (2011) 42.
15. C. Liu, R. Bai, L. Hong, Diethylenetriamine–grafted poly(glycidyl methacrylate) adsorbent for effective copper ion adsorption, J. Colloids Interf. Sci., 303 (2006) 99.

16. R. Say, B. Garipcan, S. Emir, S. Patır, A. Denizli, Preparation and characterization of the newly synthesized metal–complexing–ligand N–methacryloylhistidine having PHEMA beads for heavy metal removal from aqueous solutions, Macromol. Mater. Eng., 287 (2002) 539.
17. G. Bayramoğlu, M.Y. Arıca, Ethylenediamine grafted poly(glycidylmethacrylate–co–methylmethacrylate) adsorbent for removal of chromate anions, Sep. Purif. Technol., 45, (2005) 192.
18. R. Say, A. Tuncel, A. Denizli, Adsorption of Ni(II) from Aqueous Solutions by Novel Polyethyleneimine–attached Poly(p–chloromethylstyrene) beads J. Appl. Polym. Sci., 83 (2002) 2467.
19. K.A.K. Ebraheem, S.T. Hamdi, Synthesis and properties of a copper selective chelating resin containing a salicylaldox– ime group, React. Funct. Polym., 34 (1997) 5.
20. A. Üçer, A. Uyanık, Ş.F. Aygün, Adsorption of Cu(II), Cd(II), Zn(II), Mn(II) and Fe(III) ions by tannic acid immobilised activated carbon, Sep. Purif. Technol., 47 (2006) 113.
21. A. Kara, Adsorption of Cr(VI) ions onto poly(ethylene glycol dimethacrylate–1–vinil–1,2,4–triazol), J. Appl. Polym. Sci., 114 (2009) 948.
22. I. Safarik, M. Safarikova, Magnetic affinity separation of recombinant fusion proteins, Hacettepe J. Biol. Chem., 38 (2010) 1–7.
23. E.M. Szablewska, M. Safarikova, I. Safarik, Magnetic studies of ferrofluid–modified microbial cells (2010) J. Nanosci. Nanotechnol., 10 (2010) 2531.
24. I. Safarik, M. Safarikova, Magnetic nano– and microparticles in biotechnology, Chem. Papers, 63 (2009) 497.
25. H. Yavuz, A. Denizli, H. Gungunes, M. Safarikova, I. Safarik, Biosorption of mercury on magnetically modified yeast cells, (2006) Sep. Purif. Technol., 52 (2006) 253.
26. D.M. Schhulte, T.S. Rode, Thermoresponsive magnetic polymer particles as contactless controllable drug carriers, J. Magn. Magn. Mater., 302 (2006) 267.
27. S. Şenel, L. Uzun, A. Kara, A. Denizli, Heavy metal removal from synthetic solutions with magnetic beads under magnetic field, J. Macromol. Sci. Pure & Applied Chem. A, 45 (2008) 635.
28. G. Huang, H. Zhang, J.X. Shi, T.A.G. Langrish, Adsorption of chromium(VI) from queous solutions using cross–linked magnetic chitosan beads, Ind. Eng. Chem. Res., 48 (2009) 2646.
29. G. Bayramoglu, M.Y. Arıca, Adsorption of Cr(VI) onto immobilized acyrlate–based magnetic beads: isotherms, kinetics and thermodynamics study. Chem. Eng. J., 139 (2008) 20.
30. H. Li, Z. Li, T. Liu, X. Xiao, Z. Peng, L. Deng, A novel technology for biosorption and recovery hexavalent chromium in wastewater by bio–functional magnetic beads, Bioresour. Technol., 99 (2008) 6271.
31. S. Basha, Z.V.P. Murthy, B. Jha, Kinetics, Isotherms, and Thermodynamics of Hg(II) Biosorption onto Carica papaya, Ind. Eng. Chem. Res., 15 (2011) 26.
32. Y.S. Ho, Selection of optimum sorption isotherm, Carbon, 42 (2004) 2115.
33. K.V. Kumar, S. Sivanesan, Isotherm parameters for basic dyes onto activated carbon: comparison of linear and non–linear method, J. Hazard. Mater., 129 (2006) 147.
34. S.D. Faust, O.M. Aly, Adsorption processes for water treatment, Butterworths Publishers, Stoneham, MA (1987).
35. H.M.F. Freundlich, Uber die adsorption in lasugen, Z. Phys. Chem. (Leipzig), 57A (1906) 385.
36. I. Langmuir, The constitution and fundamental properties of solids and liquids. part i. Solids, J. Am. Chem. Soc., 38 (1916) 2221.
37. M.M. Dubinin, The potential theory of adsortion of gases and vapors for adsorbents with energitically nonuniform surfaces, Chem. Rev., 60 (1960) 235.
38. M.J. Temkin, V. Pyzhev, Recent modifications to Langmuir isotherms, Acta Physicochim URSS, 12 (1940) 217.
39. G. Halsey, Physical adsorption on non–uni– form surfaces, J. Chem. Phys., 16 (1948) 931.
40. O. Redlich, D.L. Peterson, A Useful Adsorption Isotherm, J. Phys. Chem., 63 (1959) 1024.
41. R. Sips, On the structure of a catalyst surface, J. Chem. Phys., 16 (1948) 490.
42. A.R. Khan, R. Ataullah, A. Al–Haddad, Equilibrium Adsorption Studies of Some Aromatic Pollutants from Dilute Aqueous Solutions on Activated Carbon at Different Temperatures, J. Colloid Interface Sci., 194 (1997) 154.
43. C.J. Radke, J.M. Prausnitz, Adsorption of organic solutes from dilute aqueous solution on activated carbon, (1972) Ind. Eng. Chem. Fundam., 11 (1972) 445.
44. J. Toth, Calculation of the BET–compatible surface area from any type I isotherms measured above the critical temperature, J. Colloid Interface Sci., 225 (2000) 378.
45. R.A. Koble, T.E. Carrigan, Adsorption isotherms for pure hydrocarbons, Ind. Eng. Chem., 44 (1952) 383.
46. W. Fritz, E.U. Schlunder, Simultaneous adsorption equilibria of organic solutes in dilute aqueous solutions on activated carbon, Chem. Eng. Sci., 29 (1974) 1279.

47. S. Kundu, A.K. Gupta, Arsenic adsorption onto iron oxide–coated cement (IOCC): Regression analysis of equilibrium data with several isotherm models and their optimization, Chem. Eng. J., 122 (2006) 93.
48. B. Unal, Z. Durmus, A. Baykal, M.S. Toprak, H. Sozeri, A. Bozkurt, Synthesis, dielectric and magnetic characteristics of poly(1–vinyl–1,2,4–triazole) (PVTri)-barium hexaferrite composite, J. Alloys Compd., 509 (2011) 8199.
49. M.R. Unnithan, V.P. Vinod, T.S. Anirudhan, Synthesis, characterizations and applications as a chromium(VI) adsorbent of amine–modified polyacrylamide–grafted coconut coir pith Ind. Eng. Chem. Res., 43 (2004) 2247.
50. F. Göde, E. Pehlivan, Removal of Cr(VI) from aqueous solution by two Lewatit–anion exchange resins, J. Hazard. Mater., B119 (2005) 175.
51. M. Jain, V.K. Garg, K. Kadirvelu, Adsorption of hexavalent chromium from aqueous medium onto carbonaceous adsorbents prepared from waste biomass, J. Environ. Manage., 91 (2010) 949.
52. F. Göde, N. Öztürk, Y. Sert, S. Bahçeli, Adsorption of Cr(VI) from Aqueous Solutions Onto Raw and Acid–Activated Reşadiye and Hançılı Clays, Spect. Letters, 43 (2010) 68.
53. P.A. Kumar, S. Chakraborty, M. Ray, Removal and recovery of chromium from wastewater using short chain polyaniline synthesized on jute fiber, Chem. Eng. J., 141 (2008) 130.
54. B. Xue, D. Tong, Y. Sun, Characterization of PVA–based magnetic affinity support for protein adsorption, Sep. Sci. Technol., 36, 2449.
55. Z. Aksu, T. Kutsal, Biosorption process for removing lead(II) ions from waste water by using vulgaris, J. Chem. Technol. Biotechnol., 52 (1991) 109.
56. A. Kara, A. Tuncel, Kinetics, isotherms and thermodynamics of lead (II) ions adsorption onto monosized porous microspheres carrying imidazole functional groups, Adsorpt. Sci. Technol., 29 (2011) 259.
57. B. Osman, A. Kara, N. Beşirli, Immobilization of Glucoamylase onto Lewis Metal Ion Chelated Magnetic Affinity Sorbent: Kinetic, Isotherm and Thermodynamic Studies, J. Macromol. Sci. Pure & Applied Chem., A48 (2011) 387.